JOURNAL OF MECHANICS OF CONTINUA AND MATHEMATICAL SCIENCES
ISSN (Online) : 2454 -7190 www.journalimcms.org ISSN (Print) 0973-8975
J. Mech. Cont.& Math. Sci., Special Issue, No.-5, January (2020) pp 95-108

HIGH VOLTAGE GAIN INTERLEAVED BOOST CONVERTER WITH ANFIS BASED MPPT CONTROLLER FORFUEL CELL BASED APPLICATIONS

Reddi Rani[1], Jithendra Gowd[2], Dharani Lakshmi[3]

[1 2 3]Department of Electrical and Electronics Engineering, Jawaharlal Nehru Technological University, Sir Mokshagundam Visvesvaraya Rd, Anantapur, Andhra Pradesh, India.

[1]rrputani@gmail.com, [2]indra.jithu@gmail.com,
[3]dharani.padma2010@gmail.com

Corresponding Author: Reddi Rani

https://doi.org/10.26782/jmcms.spl.5/2020.01.00008

Abstract

Due to extra effective control on emissions of carbon gas and economic benefits, Fuel cell EV is evolving into more favourite in the vehicle industry. Now- a-days pollution is one of the important factors to reduce for better life. This paper introduces a neural network system based MPP tracking controller to track the maximum power from the01.260-kW proton exchange membrane fuel cell (PEMFC). The proposed neural network MPPT controller utilizes an adaptive-network based fuzzy inference system (ANFIS) algorithm to track the PEMFC's maximum power point. Switching frequency, voltage-gain required high for the propulsion of fuel cell EV. A 3-phase high voltage gain with interleaved technique based boost converter is intended for the fuel cell EV system to get the maximum voltage gain. The interleaving type technique minimizes ripple in input fuel cell current and the voltage stress on the used semiconductor devices. The analysis of the performance of the Fuel cell EV system with ANFIS controller used is compared with the radial basis FN controller in Simulink/MATLAB.

Keywords: High voltage IBC, Fuel cell EV, HVG, ANFIS.

I. Introduction

Because of the pollution of environment and limited reserves of non-renewable energy sources, automobile sectors are indicating more intrigue in Fuel Cell EV (FCEV).The fast advances in engineering (power electronics) for fuel cells have given the powerful developments in Fuel cell EVs [I]&[II]. The better advantages of fuel cells are generation of pure power, maximum reliability, low noise and maximum efficiency [III].

The Paper Presented at National Conference on Recent Trends & Challenges in Engineering
Organized by Rajive Gandhi Memorial College, AP, India

Different kinds of fuel cells are available based on electrolyte used in the fuel cell. Due to fuel cells minimum working temperature and rapid start-up, PEMFCs dominate the automotive industry [IV].

The fuel cell output voltage depends on fuel cell temperature and membrane water level. Notably, voltage – current characteristics of fuel cell are non-linear. Therefore, only one single operating point with maximum output voltage and energy is available for the PEMFC system [V].

The method of peakpower tracking (MPPT) is essential to obtain peak energy value from the fuel cell under distinct working circumstances. Different MPPT techniques are available in the different literature survey such as methods of perturb & observe, Incremental conductivity (INC), practical swarm optimization (PSO), fuzzy logic (FLC) type and sliding mode controls, neural based network (NN) tracking maximum energy point (MPP)[V]-[X].

Among these Perturb & observe high power point tracking algorithm is popular, simple and easy to implement, among all available MPPT algorithms. By reducing or raising the control variable by a tiny quantity this algorithm stepsperturbs the working operating point and calculates the PEM fuel cell stack given output power, previous and later perturbation. If the power output of PEMFC improves, without interruption this algorithm steps perturbs the operational system in the similar direction, otherwise algorithm perturbs the operating system in the opposite direction. Although the P and Observe algorithm is easy and simple, its accuracy value is low at steady state due to the perturbation steps that causes the PEMFC system operating point oscillate all over the MPP and which leads to energy loss. The oscillations can be here minimized by decreasing the perturbation process step size.

However, lower step size reduces the tracking speed. In addition, INC controller is intended to enhance the PEMFC system's dynamic performance and tracking efficiency. This technique depends on the slant of power-current waveform. The slant of power and current curve is zero at the peak power point.

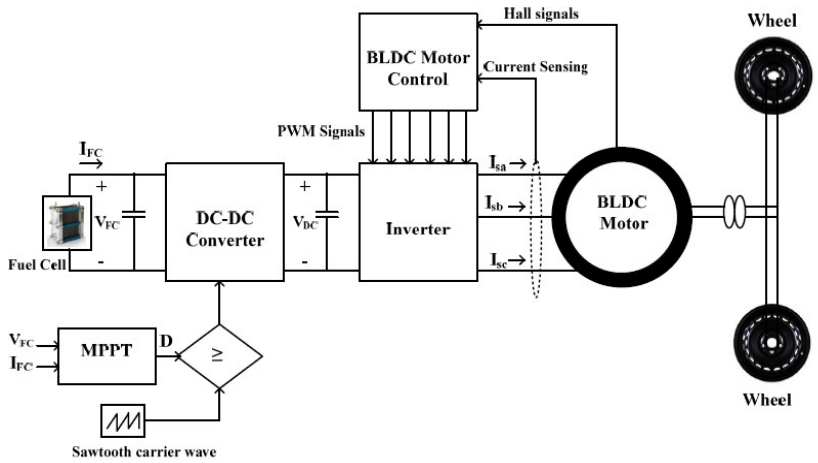

Fig 01: **Conventional configuration of fuel cell fed BLDC motor driven EV.**

The fig. 01 shows conventional connection of fuel cell with voltage source inverter through DC-DC converter fed BLDC motor. The PEMFC stack developed an unregulated minimum direct current output voltage. To reduce this problem a step-up or boost dc to dc converting converter is needed to regulate and boost up the output voltage of PEMFC.In order to achieve minimum switching stress and maximum voltage gain, this paper uses a three-phase boost converter with interleaving (IBC) for fuel cell uses and its applications.

The method of interleaving increases the fuel cell's reliability and offers high capacity. The proposed converter output voltage is supplied to the brushless dc motor through a voltage source inverter for use of starting of the electric vehicle. In FCEVs, the motor type plays a major role.

A proper motor significantly decreases the fuel cell's size and price. In the past, most car manufacturers used DC motors for electric vehicles applications. Owing to the rotating systems and brushes, DC motors have low efficiency and high maintenance costs. Due to easy high efficiency, easy control and high robustness, permanent magnet brushless DC motor is currently mostly used in fuel cell EV applications. It comprises of a fuel cell which is 1.26 kW PEMFC, IBC, MPPT controller and Inverter (VSI), Brushless DC motor and electronic commutation. The IBC three phase works as a PEMFC-VSI interface.

Three-phase connection IBC provides power through VSI to the motor type of BLDC engine. The VSI switches are regulated using BLDC motor electronic commutation. The inputs for the proposed device are PEM type fuel cell voltage (V_F), PEMFC current(I_F) and the output is duty cycle (D).The remaining paper described as follows: modeling of PEM fuel cell analyses in section II; proposed

converter modeling is explained in third (III) section; MPPT controlled techniques discussed in fourth (IV) section; Commutation in (V) section, simulation result analysis in VI section and summarized the final conclusions in section VII.

II. Modeling of the fuel cell

A proton exchange membrane FC is an electrochemical energy device that generates electricity energy by process of chemical reaction. The air and fuel are given as inputs to the fuel cell and by a chemical reaction these inputs are converted into products water product and electricity. A one fuel cell, from fig.02 consists of anode and cathode (the two electrodes) and electrolyte. The charged ions of the hydrogen fuel are separated by electrolyte.

The inputs hydrogen and oxygen given to fuel cell corresponding operation is performed and output is obtained at output side. Outputs produced are having wastages water and heat. This wastages (water and heat) not having problems of pollution. That is why present days this type of cells used for vehicle applications.

The cell used is having voltage and it is calculated by [IV], [V];

$$V_F = E_{Nerns} - V_{actl} - V_{ohmc} - V_{co} \quad (1)$$

Where in eqn (01), $E_N$is reversible (it is open-circuitvoltage) thermodynamic voltage.

The chemical reaction formula for fuel cell is described as

$$2H_2 + O_2 \rightarrow 2H_2O + \text{energy}.$$

$$V_{actl} = -[\delta_{01} + \delta_{02} T + \delta_{03} T \ln(C_{O2}) + \delta_{04} T \ln(I_{FC})] \quad (2)$$

Here δ_k (k = 01, 02, 03, and 04) is value of coefficient for everyfuel cell, C_{O2} is called as concentration content of the dissolved oxygen (O_2)at the gas or liquid interface.

The dissolved oxygen determined by using thebelow expression

$$C_{O2} = \frac{P_{O2}}{(05.08 \times 10^6) \times exp(-0498/T)} \quad (3)$$

V_{ohmc}(Ohmicbased overvoltage)is described as

$$V_{ohmic} = I_F(R_C + R_M) \quad (4)$$

Where R_M in the equation is electron flow equipment resistance and $R_C$term is the resistance of proton. Resistance (R_C)is taken as constant.

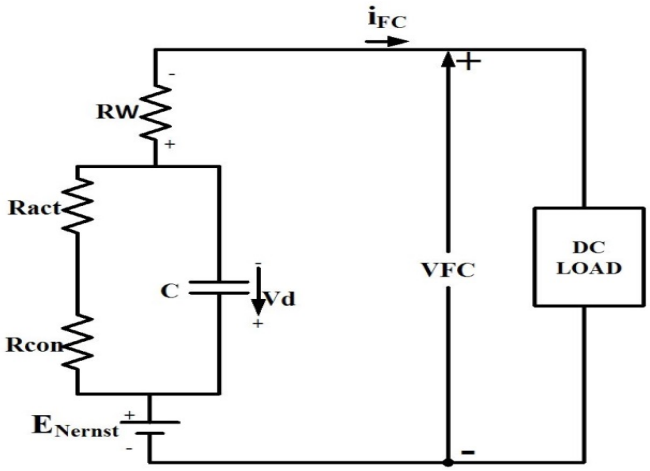

Fig 02: **Equivalent circuit of PEM fuel cell electric model.**

$$R_M = \frac{\rho_{mL}}{A} \tag{5}$$

Where,thickness of membrane is L in (cm), A represents area of membrane (cm^2).

ρ_m is the resistivityvalue symbol of membrane (Ω-cm) and formula is given in below equation.

$$\rho_m = \frac{181.6[1 + 0.03J + .062\ \ (T/0303)^2(J)02.5]}{[G - 0.6340 - \quad]exp[04.18(01 - 0303/T)]} \tag{6}$$

Form equation written above, G is content of water for membrane, T is temperature, J is described as current density term and it is,

$$J = \frac{I_{FC}}{A} \tag{7}$$

Finally, over voltage concentration V_{co} is computed from the below expression

$$V_{co} = -\frac{RT}{nF} ln\left(01 - \frac{J}{J_{max}}\right) \tag{8}$$

Where, J_{max} is peak current density and T is temperature.

The DC to DC converter input is given from the output values of the cell to balance voltage constant

across direct current link, the values for the01.26 kW PEMFC design are specified in TABLE01.

TABLE 1. **01.26 kW PEMF cell parameter specifications.**

Parameter Description	Rating
Maximum power (P_{max})	1.26 kW
Maximum voltage (V_{max})	24.23 V
Maximum current (I_{max})	52 A
Temperature (T)	55^0C
Number of cells	42
Nominal air flow rate	2400 lpm

III. Modeling of HVG boost converter

The converter used is plays a crucial role in the operation and performance of the circuit configuration. The design of the boost converter with interleaving technique is used in this paper due to advantages of technique. Converter used in proposed work consists of 3 diodes, 3 switches, 3 inductors and 3 capacitors of three phases. Fuel cell is connected as input side and inverter (VSI) connected as output side. The inputs to the converter are fuel cell current and voltage.

There are some assumptions considered for converter operation and its analysis:

i. All inductors are ideal for all phase ($L_1 = L_2 = L_3 = L$).

ii. Same value of capacitance for first and second capacitors ($C = C_1 = C_2$).

iii. The converter used in this work always operates in CCM.

iv. The current ripples in inductor and capacitor are assumedvery small.

The three switches are switched ON by the use of gate pulses having 180^0 phase shift. For second switch given one gate pulse and with the 180^o phase shift [XI] another pulse given to the first and third switches. The converter used having four modes of for operation. Under first mode of operation all the switches ON and diodes three are reverse biased. In second modeof converter operation, first and third switches ON and second switch OFF, and 1 and 3 diodes are forward biased, second diode is operated in reverse bias.

Third mode is same as first mode, three switches ON and three diodes switched OFF. In fourth mode of operation, switches 1 and 3 are ON and switch 2 OFF, diodes 1 and 3 are reverse (conduction) biased and diode 2 conducting. Based on the operation of switches and diodes in particular modes, the current through the inductors are changes based on the corresponding slops. The energy supplied by the capacitors based on modes of operation. The converter boost up the output with minimum current ripples and voltage stress.

IV. Controller design

For proposed configuration two control strategies used. One controller used for brush less DC motor operation and another controller is used for to obtainfuel cell maximum point power.

ANFIS MPPT Controller

The ANFIS is an information-driven process that represents a neural based network strategy to problem solving approximation of function.Typically, data-driven processes for ANFIS network synthesis are dependent on grouping a preparation set of function unknown numerical samples to be approximated.

For simplicity, it is assumed that there are two inputs, one output in the Fuzzy inference model system under account. The rule base includes Takagi &Sugeno's rules that is fuzzy if-then rules [XIII], as follows (Inputs x, y & z taken as v,w&u) and A,B taken as R,S) :

$$\text{If v is R and w is S then u is f(v,w)} \tag{9}$$

Where Rand S are sets of fuzzy in the antecedents, u= f(v, w) is a function of crisp in the part of consequent.
Usually f(v, w) is an input variables polynomial v and w. But it is also be any other feature that describes the system output in the fuzzy operating region roughly as indicated by the term antecedent. When f(v, w) is a value of constant, fuzzy model of zero order and it is developed which can be taken as a special step of the Mamdani type inference system [XII].If f(v, w) is considered a polynomial of 1st order, a 1st order Sugeno type fuzzy model will be developed.
For a 1st order 2 rule based Sugeno type fuzzy inference scheme the types of 2 rules, may be indicated as:

Rule 01: If v is R_1 and w is S_1 then $f_1 = p_1v + q_1w + r_1$

Rule 02: If v is R_2 and w is S_2 then $f_2 = p_2v + q_2w + r_2$

The each rule output is linear one and having input factors summed through a term of constant value in the inference system used. The average of every each rule's output is final output.Fig.03 shows the respective ANFIS structure.

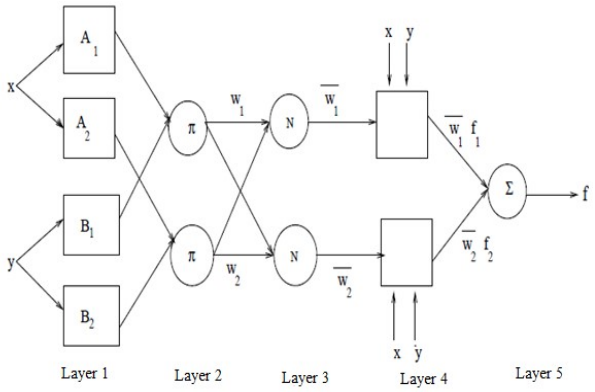

Fig03:**ANFIS based MPPT structure for fuel cell.**

This ANFIS structure's individual layers are defined below:

Layer 01: Each node n is adaptive feature with a node feature in this layer

$$O_n^1 = \mu_{A_n}(v) \qquad 10)$$

Where v is the node n input,R_n is the linguistic type variable connected with the function of node andμ_{R_n} is the MF of r_n. Usually $\mu_{R_n}(v)$ is selected as

$$\mu_{R_n}(v) = \frac{01}{1+\left[\left(\frac{v-c_n}{a_n}\right)\right]b_n} \qquad (11)$$

Where input is v and premise parameter set is $\{a_n, b_n, c_n\}$.

Layer 02: In this second layer each node is node of fixed value and it is determine the firing strength $\omega_n$of each a rule. The product of incoming signals as the output and is,

$$O_n^2 = \omega_n = \mu_{R_n}(v) \times \mu_{R_n}(w),\ n = 1,2 \qquad (12)$$

Layer 03: In this third layer each node is a fixed node, andn^{th} node output value is the normalized firing strength given by,

$$O_n^3 = \overline{\omega_n} = \frac{\omega_n}{\omega_1 + \omega_2}, \qquad n = 1,2 \qquad (13)$$

Layer 04: Node function is given by

$$O_n^4 = \overline{\omega_n} f_n = \overline{\omega_n}(P_n v + q_n w + r_n),\ n = 1,2 \qquad (14)$$

Layer 05: This layer consists of a single fixed node calculating the total output value as the calculated by adding all incoming signals, i.e.

$$overall\ output = O_n^5 = \sum_n \overline{\omega_n} f_n = \frac{\sum_n \omega_n f_n}{\sum_n \omega_n} \qquad (15)$$

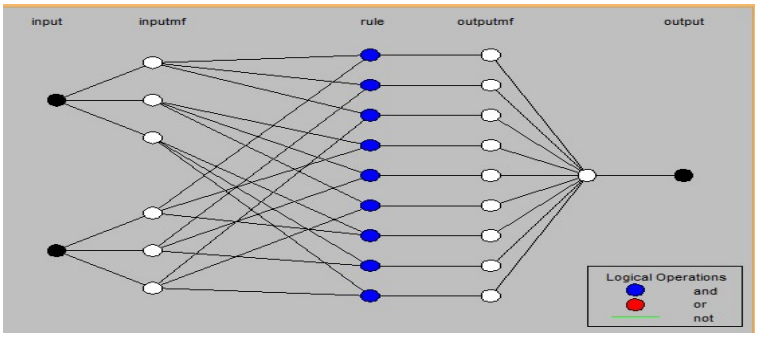

Fig04: **ANFIS structure generated in MATLAB.**

Learning Algorithm

The fig.04 shows the ANFIS model, it is notice that premise parameter values are given to this model and output response that is linear amalgamation of the consequent set.

The value of output f is given as,

$$f = \frac{\omega_{01}}{\omega_{01}+\omega_{02}} f_{01} + \frac{\omega_{02}}{\omega_{01}+\omega_{02}} f_{02} \quad (16)$$

$$= \overline{\omega_{01}} f_{01} + \overline{\omega_{02}} f_{02} \quad (17)$$

$$= (\overline{\omega_{01}}\, v)p_{01} + (\overline{\omega_{01}}\, w)q_{01} + (\overline{\omega_{01}})r_{01} + (\overline{\omega_{02}}\, v)p_{02} + (\overline{\omega_{02}}\, w)q_{02} + (\overline{\omega_{02}})r_{02} \quad (18)$$

Where consequent set parameters are named as $(p_{01}, q_{01}, r_{01}, p_{02}, q_{02}, r_{02})$.

V. Electronic commutation

The control signals given to the VSI switches are acquired from the electronic switching of the Brush less DC motor [XV].Depending on the located of the operating motor rotor, 3 hall sensors are used to produce three hall signals for each interval of 60^0.Using a decoder circuit, these produced hall sensor signals are transformed to switching operating pulses to the VSI.TABLE.2 shows the switching pulses of the voltage source inverter.

TABLE 2. **Brushless DC motor electroniccommutation switching states**

Θ (deg)	Hall Signals			Switching States					
	H_1	H_2	H_3	S_4	S_5	S_6	S_7	S_8	S_9
NA	0	0	0	0	0	0	0	0	0
0-60	1	0	1	1	0	0	1	0	0
60-120	1	0	0	1	0	0	0	0	1
120-180	1	1	0	0	0	1	0	0	1
180-240	0	1	0	0	1	1	0	0	0
240-300	0	1	1	0	1	0	0	1	0
300-360	0	0	1	0	0	0	1	1	0
NA	1	1	1	0	0	0	0	0	0

VI. Simulation results

Using the Simulink /MATLAB platform, the operation and execution of the suggested Brush less DC motor driven FCEV scheme is evaluated.To evaluate the FCEV system's dynamic response, sudden value changes in the fuel cell operating temperature are regarded as follows:
T = 0320^{o}K for a time period of 00 to 00.30sec, T= 0310^{o}K for a time period of 00.30 sec to 0.60 sec and 330^{o}K for 00.60 to 0.90 sec as shown in fig.05.

The fuel cell output values of voltage, current values and power values in waveforms at distinct temperatures are as shown in waveform fig.06. The value of power generated by the proposed fuel cell for the period 0 to 0.3 is 1090W, for 0.3 to 0.6 power is 990W and for 0.6 to 0.9 the power is 1200W. From fig.07, Observed that the simulation result of DC link values of output voltage, output current and power waveforms at distinct temperatures using RBFN.

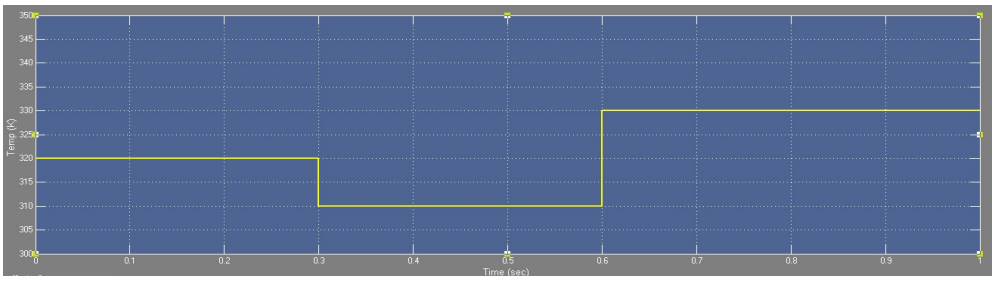

Fig. 05: **PEMFC system temperature change.**

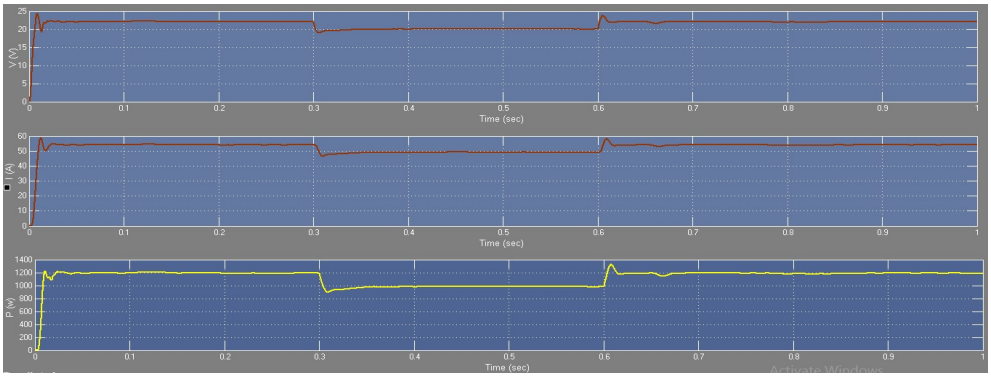

Fig 06: **Output voltage, current and power of fuel cell at different temperatures.**

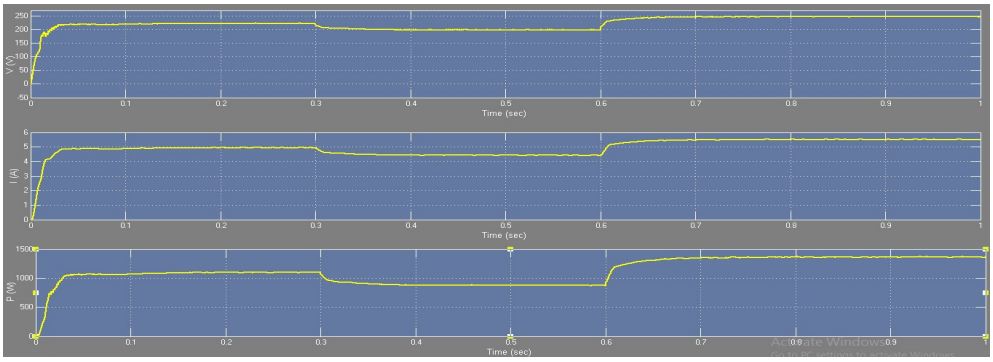

Fig 07: **Output voltage, current and power of DC link at different temperatures using RBFN.**

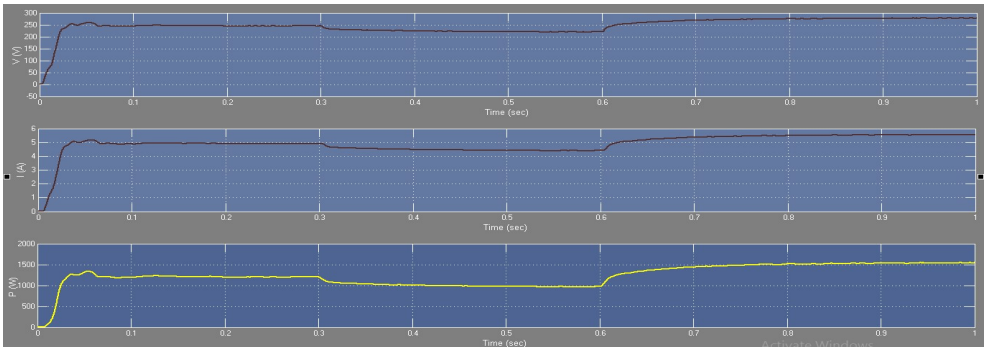

Fig 08: **Output voltage, current and power of DC link at different temperatures using ANFIS.**

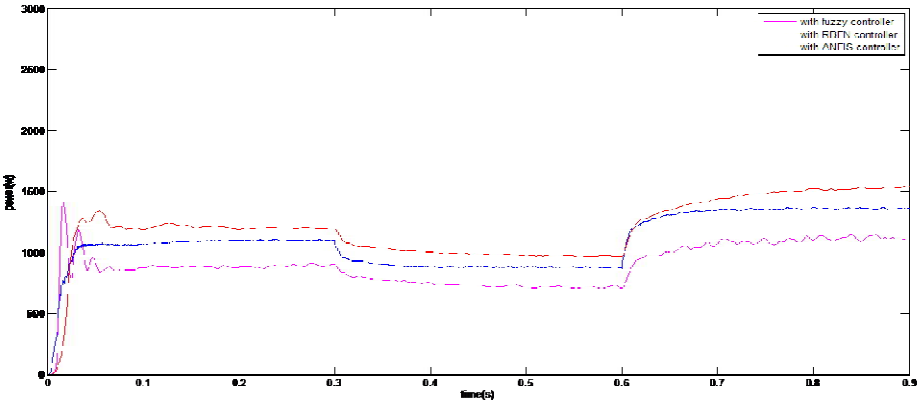

Fig 09: **Comparison of power by using fuzzy controller, RBFN Controller, ANFIS.**

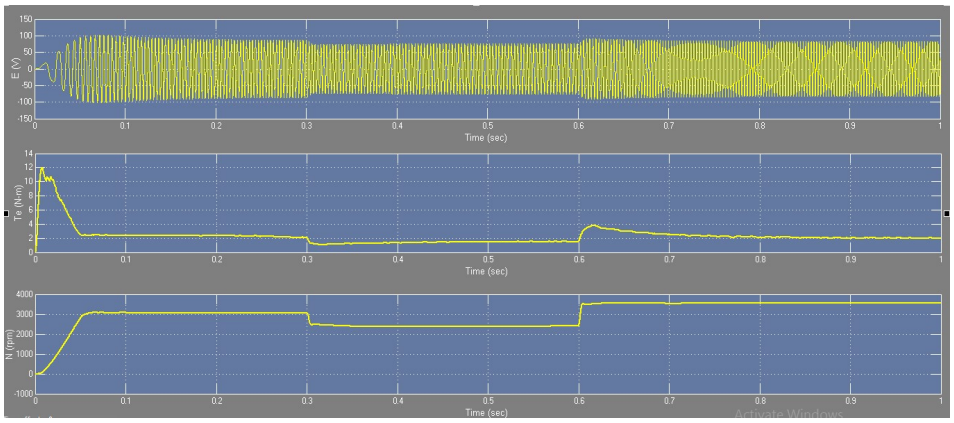

Fig 10: **Parameters of BLDC.**

The ANFIS based controller gives 1000W for 310^{o}K, 1200W for 320^{o}K and 1540W power for the 330^{o} K. fig.09 shows the performance of ANFIS,RBFN and fuzzy at different temperatures. From fig.09 observed that ANFIS based MPPT controller developed high DC link output power compared to RBFN based MPPT controller. The comparison analysisof ANFIS and RBFN is shown in TABLE 3.

The steady-state and starting characteristics at different temperatures of Brushless DC motor waveforms are as shown in fig. 10.The parameters of motor such as the back EMF (E), load torque (T_L) and electromagnetic torque (T_e) are represented at fuel cell dynamic different temperature conditions.

TABLE 3. **Comparison of ANFIS and RBFN based MPPT controllers DC link power.**

Parameter	1.26 kW PEMFC with RBFN based MPPT			1.26 kW PEMFC with ANFIS based MPPT		
Period(sec)	0 to 0.3	0.3 to 0.6	0.6 to 0.9	0 to 0.3	0.3 to 0.6	0.6 to 0.9
Fuel cell temperature (^{O}K)	320	310	330	320	310	330
DC link current(A)	4.90	4.43	5.51	4.93	4.49	5.61
DC link voltage(V)	220	198	248	245	220	275
DC link power(W)	1100	880	1360	1200	1000	1540

VII. Conclusion

In this work, a three-phase andmaximum voltage gain IBC is used for Fuel cell EV applications. The ANFIS based MPP tracking controller is designed for 01.260 kW PEMF cell for tracking peak (maximum) power from the PEMF cell. The converter used in proposed work reduces ripples in current waveform and voltage stress on the switches. At distinct temperatures of fuel cell, different performance characteristics of the motor are analyzed. The results of proposed system compared with the RBFN MPPT controller output values; comparison shows ANFIS MPPT controller obtained the peak power point value faster than RBFN controller.

References

I. A. Giustiniani, G. Petrone, G. Spagnuolo, M. Vitelli, “Low-frequency current oscillations and maximum power point tracking in grid-connected fuel-cell-based systems”, IEEE Trans Indus Electron., Vol.: 57, Issue: 6, pp. 2042-2053, 2010.

II. B. Geng, J. K. Mills, D. Sun, “Combined power management/design optimization for a fuel cell/battery plug-in hybrid electric vehicle using multi-objective particle swarm optimization”, Inter J. Automot Techn., Vol.:15, Issue: 4, pp.645-654, 2014.

III. F. Sobrino-Manzanares, A. Garrigós, “An interleaved, FPGA-controlled, multi-phase and multi-switch synchronous boost converter for fuel cell applications”, Int J of Hydrogen Enery., Vol.: 40, Issue: 36, pp. 12447-56, 2015.

IV. H. Hemi, J. Ghouili, A. Cheriti, "A real time fuzzy logic power management strategy for a fuel cell vehicle", Energy Convers. Manag., Vol.: 80, pp. 63-70, 2014.

V. H. J. Chiu, L.W. Lin, "A bidirectional DC–DC converter for fuel cell electric vehicle driving system", IEEE Trans Power Electron., Vol.21(4), pp.950-958, 2006.

VI. J. P. Ram, N. Rajasekar, M. Miyatake, "Design and overview of maximum power point tracking techniques in wind and solar photovoltaic systems", Renew Sustain Energy Rev., Vol. 73, pp. 1138-1159, 2017.

VII. K. J. Reddy, N. Sudhakar, "High voltage gain interleaved boost converter with neural network based MPPT controller for fuel cell based electric vehicle applications", IEEE Access, Vol.: 6, 2018:3899e908.

VIII. K. Kumar, N. R. Babu, K. R. Prabhu, "Design and Analysis of RBFN-Based Single MPPT Controller for Hybrid Solar and Wind Energy System", IEEE Access., Vol. 5, pp.15308-15317, 2017.

IX. M. Buragohain, C. Mahanta, "ANFIS Modeling of Nonlinear Systems based on Subtractive Clustering and V-fold Technique", Proceedings of IEEE Annual India Conference, New Delhi, 2006.

X. M. Buragohain, C. Mahanta, " Full Factorial Design based ANFIS Model for Complex Systems", Proceedings of IEEE Annual India Conference, New Delhi, 2006.

XI. N. Mebarki, T. Rekioua, Z. Mokrani, D. Rekioua, S.Bacha, "PEM fuel cell/battery storage system supplying electric vehicle", Int. J. of Hydrogen Enery., Vol.: 41, Issue: 45, pp.20993-21005, 2016.

XII. S. Abdi, K. Afshar, N. Bigdeli, S. Ahmadi, "A novel approach for robust maximum power point tracking of PEM fuel cell generator using sliding mode control approach", Int. Jou. Elec. Sci., pp. 4192-4209, 2012.

XIII. S. Saravanan, N. R. Babu, "Maximum power point tracking algorithms for photovoltaic system–A review", Renew Sustain Energy Rev., Vol.: 57, pp. 192-204, 2016.

XIV. T. Esram, P. L. Chapman, "Comparison of photovoltaic array maximum power point tracking techniques", IEEE Trans Energy Conver., Vol.: 22, Issue: 2, pp.439-49, 2007.

XV. V. Bist, B. Singh, "Reduced sensor configuration of brushless DC motor drive using a power factor correction-based modified-zeta converter", IET Power Electron., Vol.: 7, Issue: 9, pp. 2322-2335, 2014.